Cervical spinal cord atrophy and Alzheimer's disease.

Roberta Maria Lorenzi [1], Fulvia Palesi [2,3], Gloria Castellazzi [1,4], Paolo Vitali[3], Nicoletta Anzalone[5], Sara Bernini[6], Elena Sinforiani[6], Giuseppe Micieli[7], Alfredo Costa[2,8], Egidio D'Angelo [2,9], and Claudia A.M. Gandini Wheeler-Kingshott [4,2,10]

[1]Department of Electrical, Computer and Biomedical Engineering, University of Pavia, Pavia, Italy,

[2]Department of Brain and Behavioral Sciences, University of Pavia, Pavia, Italy,

[3]Neuroradiology Unit, Brain MRI 3T Research Center, IRCCS Mondino Foundation, Pavia, Italy,

[4]Queen Square MS Centre, Department of Neuroinflammation, UCL Queen Square Institute of Neurology, Faculty of Brain Sciences, University College London, London, United Kingdom,

5Universita Vita e Salute, S Raffaele hospital Milan

[6]Laboratory of Neuropsychology, IRCCS Mondino Foundation, Pavia, Italy,

[7]Department of Emergency Neurology, IRCCS Mondino Foundation, Pavia, Italy,

[8]Unit of Behavioral Neurology, IRCCS Mondino Foundation, Pavia, Italy,

[9]Brain connectivity center (BCC), IRCCS Mondino Foundation, Pavia, Italy,

[10]Brain MRI 3T Research Center, IRCCS Mondino Foundation, Pavia, Italy

Abstract

Objective: Brain atrophy is an established biomarker for dementia. We hypothesise that spinal cord atrophy is an important in vivo imaging biomarker for neurodegeneration associated with dementia.
Methods: 3DT1 images of 31 Alzheimer's disease (AD) and 35 healthy control (HC) subjects were processed to calculate volumes of brain structures and cross-sectional area (CSA) and volume (CSV) of the cervical cord (per vertebra as well as the C2-C3 pair (CSA23 and CSV23)). Correlated features ($\rho>0.7$) were removed, and best subset identified for patients' classification with the Random Forest algorithm. General linear model regression was used to find significant differences between groups ($p<=0.05$). Linear regression was implemented to assess the explained variance of the Mini Mental State Examination (MMSE) score as dependent variable with best features as predictors.
Results: Spinal cord features were significantly reduced in AD, independently of brain volumes. Patients classification reached 76% accuracy when including CSA23 together with volumes of hippocampi, left amygdala, white and grey matter, with 74% sensitivity and 78% specificity. CSA23 alone explained 13% of MMSE variance.

Discussion: Our findings reveal that C2-C3 spinal cord atrophy contributes to discriminate AD from HC. Results show that CSA23 has a considerable weight in classification tasks warranting further investigations.

Introduction

Dementia is one of the most debilitating cognitive neurodegenerative disorders affecting the central nervous system in elderly people and having a significant impact on daily life activities. Moreover, with an ageing population the incidence of dementia is growing. Clinically, several forms of dementia-like diseases that differently impair multiple cognitive and behavioral domains are defined. Alzheimer's disease (AD) is the most common cause of dementia and it is responsible for 60% to 80 % of cases worldwide[1] .

It is known that AD is associated with an extracellular deposit of β-amyloid plaques in the brain and cerebral vessels, but also to the presence of intracellular neurofibrillary tangles, which appear like paired helical filaments with hyperphosphorylated tau proteins. Tau tangles have been identified as the cause of cortical neurons' degeneration while β-amyloid oligomers have an important role in synaptic impairment, hence β-amyloid plaques deposition is suggested to raise later during the AD progression[2,3].

This neuronal degeneration explained by pathophysiology leads to macroscopic atrophy of specific brain structures, such as the hippocampi and the medial temporal lobes [4], which can be detected using Magnetic Resonance Imaging (MRI) techniques. Indeed, several MRI studies have demonstrated significant atrophy of white matter, gray matter and specific brain structures such as the hippocampi, thalami and amygdalae in AD patients suggesting that these structures are informative in identifying dementia disorders[5,6]. Indeed, hippocampi have been proposed as in vivo non-invasive imaging biomarkers of AD while other structures may be useful in distinguishing between different subtypes of dementia[7].

Recently, numerous MRI investigations have tried to identify new in vivo biomarkers for dementia and other neurological diseases. Optical Coherence Tomography studies have been used to assess that retinal ganglion cell degeneration can be associated to early stages of AD. Previous studies of other diseases associated with neurodegeneration, such as multiple sclerosis[8], amyotrophic lateral

sclerosis[9], and spinal cord injury[10], have revealed that atrophy of the spinal cord is indicative of widespread alterations of the central nervous system and might be considered as a relevant imaging biomarker in a wider range of neurodegenerative diseases. Nevertheless, this kind of alteration has never been investigated and reported in dementia patients. Hence, the main aim of the present work was to assess for the first time -to the best of our knowledge- whether spinal cord volume is significantly reduced in AD patients compared to healthy controls (HC), hypothesizing that the neurodegeneration typical of AD significantly spreads to all components of the central nervous system. Furthermore, in case of a positive outcome, it would be important to quantify the role of spinal cord features in distinguishing between AD and HC to drive design of future studies. We propose to do so by a machine learning approach for features selection, that is increasingly applied to improve diagnostic accuracy by quantitative imaging[11,12].

Materials and Methods

Subjects

A total of 66 subjects including 31 AD patients and 35 HC, as a reference group, were analyzed. 7 subjects (4 HC and 3 AD) were excluded from the study due to post-processing issues.

Inclusion criteria for patients were: clinical diagnosis of dementia on the basis of the Diagnostic and Statistical Manual of Mental Disorders (DSM-5) criteria[13], Mini-Mental State Examination (MMSE) score[14] below 24 and age above 60 years. Exclusion criteria comprised the presence of at least one of the following: epilepsy or isolated seizures, major psychiatric disorders over the previous 12 months, pharmacologically treated delirium or hallucinations, ongoing alcoholic abuse, acute ischemic or hemorrhagic stroke, known intracranial lesions, and systemic causes of subacute cognitive impairment[15]. Diagnosis of AD was made according to the criteria of the National Institute of Neurological and Communicative Disorders and Stroke and Alzheimer's Disease and Related Disorders Association (NINCDS-ADRDA) workgroup[16]. HC were enrolled on a voluntary basis among subjects with MMSE score above 27 and attending a local third age university

(University of Pavia, Information Technology course) or included in a program on healthy ageing (Fondazione Golgi, Abbiategrasso, Italy).

The study was accomplished in accordance with the Declaration of Helsinki and with the approbation of the local ethic committee of the IRCCS Mondino Foundation, upon signature of the written informed consent by the subjects.

MRI Acquisition

High resolution 3D T1-weighted(3DT1-w) MR images were acquired using a Siemens MAGNETOM Skyra3T(Siemens AG, Erlangen, Germany) with software version NUMARIS/4(syngo MR D13C version) and a receiving head-coil with 32 channels.

Scan parameters were[7]: TR=2300ms, TE=2.95ms, TI=900 ms, flip angle=9degrees, field of view (FOV)=269x252mm, acquisition matrix=256x240, in-plane resolution=1.05x1.05mm, slice thickness=1.2 mm, and 176 sagittal slices. The FOV, in feet-to-head direction, was set to cover the entire brain and cervical cord up to the C5 vertebra in all subjects.

Spinal Cord analysis

For each subject, the 3DT1-w volume was resized removing the brain and centering the FOV on the spine. Once a single volume of interest(VOI) comprising the same spinal cord regions for each 3DT1-w was defined(matrix=176x240x96 voxels), the process was automatized for the whole dataset. The resized 3DT1-w volumes were analyzed with the Spinal Cord Toolbox(http://sourceforge.net /projects/spinalcordtoolbox), an open source software specifically developed to elaborate spinal cord images, to extract features of the C1-C5 vertebrae.

The spinal cord was segmented with the *propseg* algorithm[17] and manually labelled[18] to identify all vertebrae separately[19](Figure 1). Mean cross-sectional area (CSA) and volume (CSV) were calculated for each vertebra and for the C2-C3 pair[20,21](CSA23 and CSV23), given the known sensitivity of this combined level to disease severity[22].

Brain atrophy analysis

3DT1-w images were segmented into white matter (WM), gray matter (GM) and cerebrospinal fluid (CSF) using SPM12(https://www.fil.ion.ucl.ac.uk/spm/software/spm12)[23], while left (L) and right (R) hippocampi (LHip and RHip), thalami (LThal and RThal) and amygdalae (LAmy and RAmy) were segmented using FIRST (FSL, https://fsl.fmrib.ox.ac.uk/fsl/fslwiki/FIRST)[24] (Figure 2).

WM, GM and all other brain structures volumes were calculated in mm^3. Total intracranial volume, as the sum of WM, GM and CSF, was also calculated to account for different brain sizes.

Machine learning analysis

Classification between AD and HC was performed using a machine learning approach implemented with Orange(https://orange.biolab.si/).

A total of 22 features were extracted from the above MRI morphometric analysis. Given the large number of parameters extracted compared to the sample size of our AD and HC groups, a feature reduction approach was adopted in order to control for overfitting issues. The Spearman correlation coefficient[25] was obtained in Matlab between pairs of all calculated metrics. When pairs of metrics had a correlation coefficient greater than 0.7, one metric was kept while the other was eliminated.

Ranking was implemented with the ReliefF algorithm[26] on the uncorrelated features to identified the best subset able to classify AD from HC, and particularly to investigate the contribution of spinal cord metrics to the task. In order to identify a unique subset of features, 30% of instances was employed for ranking. Data were normalized by span to avoid a polarization of the results due to the different scale of features, as for WM compared to CSA. The remaining 70% of instances was further divided into 70% for the Random Forest algorithm application and 30% to test its classification accuracy($CA=\frac{TruePositive+TrueNegative}{TruePositive+FalseNegative+TrueNegative+FalsePositive}$),

sensitivity($Sens=\frac{TruePositive}{TruePositive+FalseNegative}$) and specificity($Spec=\frac{TrueNegative}{TrueNegative+FalsePositive}$), using the previously-identified best features.

Among several machine learning algorithms, RF was selected for its robustness against a reduced number of input features and the capacity to weight features runtime, providing features relevance in a classification task[27,28]. The Receiving Operating Characteristics (ROC) curve was then obtained to visually discriminate between AD and HC and the Area Under the Curve was also calculated to quantify the overall ability of RF to discriminate between AD and HC.

Statistical analysis

Statistical tests were performed using the Statistical Package For Social Sciences (SPSS) software, version 21 (IBM, Armonk, New York). All continuous data were tested for normality using a Shapiro-Wilk test[29]. Age and MMSE were compared between AD and HC using a two-tailed Kruskal-Wallis test[30] while gender was compared using a chi-squared test[31]. A multivariate regression model with gender, age and total intracranial volume as covariates was used to compare all morphometric metrics between AD and HC. Two-sided $p<0.05$ was considered statistically significant.

Furthermore, to assess the power of the best features in explaining the variance of the MMSE, a linear regression model was implemented using the MMSE score as the dependent variable and the best features as predictors. These independent features were used in two ways: i) each predictor was used alone to determine its specific contribution to MMSE; ii) all features were used in a backward approach to identify which of them explained the greatest percentage of MMSE variance. A threshold of $p<0.01$(two-tailed) was considered statistically significant.

Results

Subjects

Population demographics and neuropsychological scores are reported in Table 1. Significant differences were found in MMSE between HC and AD patients.

Morphometric changes in AD patients

All results are reported in Table 2 and Table 3. AD patients compared to HC showed atrophy in all brain structures. Moreover, all patients for all investigated spinal cord segments showed reduced CSA at all vertebral levels, while CSV was significantly reduced only in correspondence of vertebrae C1 and C2.

AD classification based on morphometric data

Results of the correlation analysis are reported in Figure 3, and show that brain volumes are not significantly correlated with any spinal cord metrics.

Features that were considered independent from each other and that were entered in the feature selection analysis are reported in Table 4. The best features selected by the RF algorithm for the AD versus HC classification task are reported in Table 5 and include**:** RHip, WM, LAmy, LHip, CSA23, GM. Interestingly, CSA23 was identified as one of the most informative features to distinguish AD patients from HC. RF outcomes are reported in Table 6 and showed that the classification accuracy of AD patients is 76%, sensitivity 74% and specificity 78%. The Area Under Curve(AUC) percentage reaches 86%, showing a remarkable classification performance of the RF algorithm to distinguish AD from HC subjects. Moreover, it is noticeable that the hippocampi have dominant weight, but that there is a relevant contribution to the classification from CSA23.

MMSE and morphometric data relationship

The combination of the six best features, including WM, RHip, LHip, LAmy, CSA23 and GM, explained 44% of the overall variance of the MMSE. The function equation describing the linear model obtained by the regression analysis included the following terms with their weights: 0.329*LHip-0.145*RHip+0.145*LAmy+0.064*CSA23-0.227*GM+0.557*WM. The MMSE explained variance was progressively reduced by simplifying the model, i.e. removing one or more predictors, as shown in Table 7. Each separate feature significantly ($p<0.005$) explained a percentage of MMSE variance ranging between 13% to 36%. The feature that most explains MMSE variance was the WM volume(36%), with CSA explaining 13%.

Discussions

The present work is pioneering the investigation of spinal cord alterations in patients with dementia, and in particular with AD, a major neurodegenerative disease. Previous studies have reported spinal cord atrophy in patients with neurological diseases[32,33], such as multiple sclerosis, but to date no studies have explored the existence of a volumetric loss of spinal cord tissue in dementia. Post mortem studies of AD patients will be needed to confirm the source of such findings, although at first one could imagine that any change in CSA and CVS could be the result of retrograde Wallerian degeneration from the cerebral cortex[34]. It cannot be excluded, though, that alterations in spinal cord morphometric measurements (CSA and CSV) in AD is the result of primary retrogenesis linked to myelin and axonal pathology. It is indeed very significant that a recent study of the 5xFAD animal model of AD shows amyloid plaques accumulation in the spinal cord tissue, with a particular concentration at cervical level and a time dependent accumulation that starts 11 weeks from onset; interestingly, the same study found independent and extensive mielynopathy, while the motorneurons count at 6 months was not altered compared to the wild type[35]. While we cannot be conclusive on the mechanisms of spinal cord atrophy in AD, our results are intriguing and calling for larger studies of prodromic subjects to be followed over time.

Evaluating spinal cord alterations in humans in vivo is challenging due to technical and anatomical constrains. The most important technical limitation is related to image quality that may be affected by wrong subject positioning inside the scanner, individual subject's neck curvature or subject's motion. Furthermore, the spinal cord is a small structure and optimized sequences with reduced FOV and appropriate alignment should be used to obtain reproducible results[36]. Dedicated acquisition protocols would also allow one to analyse specific alterations of spinal cord GM and WM. Despite these limitations, previous studies have demonstrated that it is possible to use volumetric brain 3DT1-w data, often acquired as part of neurological examinations, for spinal cord features extraction[37,38]. These are the scans that were used for this first study and results show that

spinal cord morphometry, as measured by CSA and CSV, is significantly altered in AD, showing considerable neurodegeneration of the order of 10% compared to HC spinal cord volumes. Moreover, our results indicate that the spinal cord CSA23 contributes significantly to discriminate between HC and AD patients. Usually, only atrophy of brain regions is investigated in dementia[39,40] but our findings reveals that a better discriminative power is achievable combining information of both brain and spinal cord structures. In light of the only animal model study reported to date[35], which shows that C2-C3 is selectively affected by greater morphological alterations our results become of significant value.

It is well known that hippocampal atrophy is a key feature to detect dementia and is considered a biomarker of AD progression[41]; our results are consistent with this as both hippocampi are picked up as top features for the classification task. Moreover, it has now been recognized that other brain structures play a key role to identify AD patients and to distinguish between different subtypes of dementia[7]. Our results are, indeed, indicating that patients present significantly different brain volumes with respect to HC, and all segmented brain structures, except for the right amygdala, are statistically significantly atrophic in AD. In this context, though, our work demonstrates that volumes of all cervical vertebral segments are reduced in AD, with only the CSV of the first and second vertebrae being significantly atrophic with respect to HC. These results are coherent with results obtained for cerebral structures and suggest the existence of a remarkable reduction in the volume of spinal cord in dementia. This hypothesis is further supported by significant CSA reduction for all vertebrae in patients. Moreover, the fact that CSA23 is particularly sensitive to pathological changes in AD is in accordance with other studies in neurodegenerative diseases such as amyotrophic lateral sclerosis[9] and could be seen as a corroborating evidence of significant correlation between spinal cord atrophy and neurodegeneration. Considering that the 5xFAD animal study showed that there are significant alterations in myelin microstructure, uncorrelated with the amyloid deposits, one has to be careful in interpreting these findings as purely due to axonal loss

induced by Wallerian degeneration. It is important to assert that our findings reveal the importance of spinal cord changes in the study of dementia and suggest that CSA23 should be considered as a contributing in vivo imaging biomarker to distinguish between dementia patients and HC.

Few recent studies have combined several MRI findings with machine learning approaches to attempt the classification of dementia subtypes and prediction of disease progression. Accuracy of about 80%[42,43] was achieved when AD and HC were classified while more fluctuating results were reported when more subtypes of dementia were considered. In the present study a RF algorithm with the "leave-one-out" approach was chosen to discriminate between AD and HC because RF is robust with small numbers of subjects and performs features weighting runtime with good sensitivity and specificity. Our findings has shown that spinal cord morphometric measures (CSA and CSV) alone cannot directly discriminate between AD and HC, but CSA23 was identified as one of the six best features useful to distinguish between these groups of subjects. Classifier accuracy was good and reached its best performance, around 76%, when both volume of brain structures, such as LHip, RHip, WM and GM, and CSA23 were included in the classification procedure. In addition, the ROC curve between AD and HC (shown in Figure 4) reported high performance with AUC of 86%. The RF sensitivity and specificity, of 74% and 78% respectively, showed a remarkable ability in correcting identify healthy and pathological cases. Furthermore, the RF feature weighting (reported in Table 6) demonstrated that CSA23 had a considerable weight in the classification procedure, for example higher than GM, highlighting that it should be considered as an additional biomarker together with the more conventional volumes of subcortical regions[31]. These results indicate the yet unexplored potential influence that spinal cord features can play in the diagnosis of dementia.

Finally, our data shows that also clinical aspects of AD are partially explained by spinal cord atrophy. Given the exploratory nature of the present study, in absence of specific motor and sensory tests, it was decided to assess whether spinal cord atrophy could be correlated with the variance of

the MMSE, which is a global test, clinically used to assess AD severity. Indeed, 43% of the MMSE variance was explained with a multiple regression model implemented with all the best features included as independent variables, whereas CSA23 alone explained 13% of the MMSE variance. Targeted and well-designed imaging studies should investigate the involvement of the spinal cord at different stages of AD and in different types of dementia to explore its full clinical potentials. It is essential to promote multi-modal studies that can disentangle the contribution of myelin, amyloid accumulation, axonal swelling and axonal loss to spinal cord alterations in neurodegenerative diseases. Post-mortem studies of human tissue will be key to understand mechanisms of involvement of the spinal cord.

In conclusion, the present work can be considered a milestone because for the first time it demonstrates in a cohort of AD and HC subjects the contribution of spinal cord atrophy to explain clinical indicators of dementia and to improve disease classification, opening also mechanistic questions for future studies.

Acknowledgements

We thank University of Pavia and Mondino Foundation (Pavia, Italy) for funding; The UK Multiple Sclerosis Society and UCL-UCLH Biomedical Research Centre for ongoing support of the Queen Square MS Centre. CGWK receives funding from ISRT, Wings for Life and the Craig H. Neilsen Foundation(the INSPIRED study), from the MS Society(#77), Wings for Life(#169111), Horizon2020(CDS-QUAMRI, #634541). This research has received funding from the European Union's Horizon 2020 Framework Programme for Research and Innovation under the Specific Grant Agreement No.785907(Human Brain Project SGA2) for the work of FP and ED. ECTRIMS and the Multiple Sclerosis International Federation(MSIF) supported the work of GC with funding (ECTRIMS Postdoctoral Research Fellowship Program, MSIF Du Pré grant).

Authorship

CGWK, ED, FP and RL conceptualized the study. FP and RL designed and performed the analyses with support from GC. PV and NA acquired all MRI data. ES and SB acquired all neuropsychological data helping for data interpretation. AC, ES and GM enrolled all patients and performed all clinical evaluations. CGWK and ED provided support and guidance with data interpretation with clinical contribution of all physicians. CGWK, FP and RL wrote the manuscript, with comments from all other authors.

Conflict of interest

The authors declare that the research was conducted in the absence of any commercial or financial relationship that could be construed as a potential conflict of interest.

References

1. Kumar A, Singh A, Ekavali. A review on Alzheimer's disease pathophysiology and its management: An update [Internet]. Pharmacol. Reports 2015;67(2):195–203.Available from: http://dx.doi.org/10.1016/j.pharep.2014.09.004

2. Song H-L, Shim S, Kim D-H, et al. beta-Amyloid is transmitted via neuronal connections along axonal membranes. Ann. Neurol. 2014;75(1):88–97.

3. Šimić G, Babić Leko M, Wray S, et al. Tau protein hyperphosphorylation and aggregation in alzheimer's disease and other tauopathies, and possible neuroprotective strategies. Biomolecules 2016;6(1):2–28.

4. Scher AI, Xu Y, Korf ESC, et al. Hippocampal morphometry in population-based incident Alzheimer's disease and vascular dementia: The HAAS. J. Neurol. Neurosurg. Psychiatry 2011;82(4):373–376.

5. Stonnington CM, Chu C, Klöppel S, et al. Predicting clinical scores from magnetic resonance

scans in Alzheimer's disease [Internet]. Neuroimage 2010;51(4):1405–1413.Available from: http://dx.doi.org/10.1016/j.neuroimage.2010.03.051

6. Pini L, Pievani M, Bocchetta M, et al. Brain atrophy in Alzheimer's Disease and aging [Internet]. Ageing Res. Rev. 2016;30:25–48.Available from: http://dx.doi.org/10.1016/j.arr.2016.01.002

7. Palesi F, De Rinaldis A, Vitali P, et al. Specific patterns of white matter alterations help distinguishing Alzheimer's and vascular dementia. Front. Neurosci. 2018;12(APR)

8. Liu Z, Yaldizli Ö, Pardini M, et al. Cervical cord area measurement using volumetric brain magnetic resonance imaging in multiple sclerosis [Internet]. Mult Scler Relat Disord 2015;4(1):52–57.Available from: http://dx.doi.org/10.1016/j.msard.2014.11.004

9. Antonescu F, Adam M, Popa C, Tuță S. A review of cervical spine MRI in ALS patients. [Internet]. J. Med. Life 2018;11(2):123–127.Available from: http://www.ncbi.nlm.nih.gov/pubmed/30140318%0Ahttp://www.pubmedcentral.nih.gov/articlerender.fcgi?artid=PMC6101680

10. Grussu F, Schneider T, Tur C, et al. Neurite dispersion: a new marker of multiple sclerosis spinal cord pathology? Ann Clin Transl Neurol 2017;4(9):663–679.

11. Dauwan M, van der Zande JJ, van Dellen E, et al. Random forest to differentiate dementia with Lewy bodies from Alzheimer's disease. Alzheimer's Dement. (Amsterdam, Netherlands) 2016;4:99–106.

12. Mirzaei G, Adeli A, Adeli H. Imaging and machine learning techniques for diagnosis of Alzheimer's disease. Rev. Neurosci. 2016;27(8):857–870.

13. Association AP. Diagnostic and statistical manual of mental disorders (DSM-5®). American Psychiatric Pub; 2013.

14. Folstein MF, Folstein SE, McHugh PR. "Mini-mental state": A practical method for grading

the cognitive state of patients for the clinician [Internet]. J. Psychiatr. Res. 1975;12(3):189–198.[cited 2019 Jan 15] Available from: https://www.sciencedirect.com/science/article/pii/0022395675900266?via%3Dihub

15. Geschwind MD, Shu H, Haman A, Sejvar JJ. NIH Public Access. Ann Neurol. 2009;64(1):97–108.

16. McKhann GM, Knopman DS, Chertkow H, et al. NIH Public Access. Alzheimers Dement 2011;7(3):263–269.

17. Yiannakas MC, Mustafa AM, De Leener B, et al. Fully automated segmentation of the cervical cord from T1-weighted MRI using PropSeg: Application to multiple sclerosis [Internet]. Neuroimage 2016;10:71–77.Available from: http://dx.doi.org/10.1016/j.nicl.2015.11.001

18. Ullmann E, Pelletier Paquette JF, Thong WE, Cohen-Adad J. Automatic Labeling of Vertebral Levels Using a Robust Template-Based Approach. Int. J. Biomed. Imaging 2014;2014

19. Dupont SM, De Leener B, Taso M, et al. Fully-integrated framework for the segmentation and registration of the spinal cord white and gray matter [Internet]. Neuroimage 2017;150(August 2016):358–372.Available from: http://dx.doi.org/10.1016/j.neuroimage.2016.09.026

20. De Leener B, Mangeat G, Dupont S, et al. Topologically preserving straightening of spinal cord MRI. J. Magn. Reson. Imaging 2017;46(4):1209–1219.

21. Coulon O, Hickman SJ, Parker GJ, et al. Quantification of spinal cord atrophy from magnetic resonance images via a B-spline active surface model. Magn. Reson. Med. 2002;47(6):1176–1185.

22. D'Angelo E, Mazzarello P. MRI observation of hippocampal degeneration in Alzheimer's

disease: a forgotten case. Funct Neurol 2013;28(3):245–246.

23. Penny W, Flandin G, Trujillo-Barreto N. CHAPTER 25 - Spatio-temporal models for fMRI [Internet]. In: FRISTON K, ASHBURNER J, KIEBEL S, et al., editors. Statistical Parametric Mapping. London: Academic Press; 2007 p. 313–322.Available from: http://www.sciencedirect.com/science/article/pii/B9780123725608500255

24. Patenaude B, Smith SM, Kennedy DN, Jenkinson M. A Bayesian model of shape and appearance for subcortical brain segmentation [Internet]. Neuroimage 2011;56(3):907–922.Available from: http://dx.doi.org/10.1016/j.neuroimage.2011.02.046

25. Spearman C. The proof and measurement of association between two things. Am. J. Psychol. 1904;15(1):72–101.

26. Urbanowicz RJ, Meeker M, La Cava W, et al. Relief-based feature selection: Introduction and review. J. Biomed. Inform. 2018;85:189–203.

27. Goel E, Abhilasha E. Random Forest: A Review. Int. J. Adv. Res. Comput. Sci. Softw. Eng. 2017;7(1):251–257.

28. Breiman L. Random Forests [Internet]. Mach. Learn. 2001;45(1):5–32.Available from: https://doi.org/10.1023/A:1010933404324

29. Shapiro SS, Wilk MB. An Analysis of Variance Test for Normality (Complete Samples) [Internet]. Biometrika 1965;52(3/4):591–611.Available from: http://www.jstor.org/stable/2333709

30. Kruskal WH, Wallis WA. Use of Ranks in One-Criterion Variance Analysis [Internet]. J. Am. Stat. Assoc. 1952;47(260):583–621.Available from: http://www.jstor.org/stable/2280779

31. Pearson K. X. On the criterion that a given system of deviations from the probable in the case of a correlated system of variables is such that it can be reasonably supposed to have arisen

from random sampling [Internet]. London, Edinburgh, Dublin Philos. Mag. J. Sci. 1900;50(302):157–175.Available from: https://doi.org/10.1080/14786440009463897

32. Okuda DT, Melmed K, Matsuwaki T, et al. Central neuropathic pain in MS is due to distinct thoracic spinal cord lesions. Ann. Clin. Transl. Neurol. 2014;1(8):554–561.

33. Azodi S, Nair G, Enose-Akahata Y, et al. Imaging spinal cord atrophy in progressive myelopathies: HTLV-I-associated neurological disease (HAM/TSP) and multiple sclerosis (MS). Ann. Neurol. 2017;82(5):719–728.

34. Alves GS, Oertel Knochel V, Knochel C, et al. Integrating retrogenesis theory to Alzheimer's disease pathology: insight from DTI-TBSS investigation of the white matter microstructural integrity. Biomed Res. Int. 2015;2015:291658.

35. Chu T-H, Cummins K, Sparling JS, et al. Axonal and myelinic pathology in 5xFAD Alzheimer's mouse spinal cord. PLoS One 2017;12(11):e0188218.

36. De Leener B, Lévy S, Dupont SM, et al. SCT: Spinal Cord Toolbox, an open-source software for processing spinal cord MRI data [Internet]. Neuroimage 2017;145(October 2016):24–43.Available from: http://dx.doi.org/10.1016/j.neuroimage.2016.10.009

37. Fonov VS, Le Troter A, Taso M, et al. Framework for integrated MRI average of the spinal cord white and gray matter: the MNI-Poly-AMU template. Neuroimage 2014;102 Pt 2:817–827.

38. Levy S, Benhamou M, Naaman C, et al. White matter atlas of the human spinal cord with estimation of partial volume effect. Neuroimage 2015;119:262–271.

39. Štepán-Buksakowska I, Szabó N, Horínek D, et al. Cortical and Subcortical Atrophy in Alzheimer Disease: Parallel Atrophy of Thalamus and Hippocampus [Internet]. Alzheimer Dis. Assoc. Disord. 2014;28(1)Available from: https://journals.lww.com/alzheimerjournal/Fulltext/2014/01000/Cortical_and_Subcortical_At

rophy_in_Alzheimer.10.aspx

40. Tardif CL, Devenyi GA, Amaral RSC, et al. Regionally specific changes in the hippocampal circuitry accompany progression of cerebrospinal fluid biomarkers in preclinical Alzheimer's disease. Hum. Brain Mapp. 2018;39(2):971–984.

41. O'Callaghan C, Shine JM, Hodges JR, et al. Hippocampal atrophy and intrinsic brain network dysfunction relate to alterations in mind wandering in neurodegeneration. Proc. Natl. Acad. Sci. U. S. A. 2019;

42. Waser M, Benke T, Dal-Bianco P, et al. Neuroimaging markers of global cognition in early Alzheimer's disease: A magnetic resonance imaging-electroencephalography study. Brain Behav. 2019;9(1):e01197.

43. Amoroso N, La Rocca M, Bruno S, et al. Multiplex Networks for Early Diagnosis of Alzheimer's Disease. Front. Aging Neurosci. 2018;10:365.

Figures Legend

Figure 1. Labelled vertebrae in two randomly chosen subjects: a HC subject on the left and an AD patient on the right (slice n=96, sagittal plane). Each color represents a different vertebra from C1 (yellow) to C5 (fuchsia).

Figure 2. Cerebral tissue segmentation in two randomly chosen subjects: a HC subject on the left and an AD patient on the right. Top row: WM (yellow) and GM (blue) segmentation (slice n = 126, transverse plane). Middle row: hippocampi (yellow) and amygdalae (light blue) segmentation (slice n = 123, transverse plane). Bottom row: thalami (green) segmentation (slice n = 132, transverse plane) .

Figure 3. Correlation matrix between pairs of variables, tested with the Spearman's correlation coefficient. All correlations for $p<0.5$ are set to white, correlations for $p>0.5$ are red to yellow, with yellow ($p=1$) being the strongest correlation. No spinal crod metrics are correlating with brain metrics with $p>0.7$, which is the threshold we used for extracting the set of uncorrelated features (Table 1)

Figure 4. ROC curves for AD-HC classification using Random Forest feature selection. Pathological class (AD = 1) was considered as the target class. The curve shows higher

performance (bold red line) than the majority algorithm (diagonal). TN rate is the rate of true negative and FP rate is the rate of false positives.

Tables

Table 1: Subjects' demographic and neuropsychological data

	HC (n=32)	AD (n=28)	p-value
	mean (SD)	mean (SD)	
Age [yrs]	69.4 (9.6)	73.0 (6.4)	0.138
Gender (Male [%])	51.4	56.2	0.800
MMSE	28.5 (0.2)	16.0 (1.1)	< 0.001*

Gender is expressed in Male % and compared with a Chi-square test. Age and MMSE are expressed as mean (SD) and compared with a Kruskall-Wallis test. Significance was set to p=0.05. * refers to statistically significant comparisons.

Table 2: Brain morphometric changes in AD patients

		HC (n=32)	AD (n=28)	p-value
		mean (SD)	mean (SD)	
Brain Structures (mm^2)	ICV	1573086 (144439)	1511611 (139532)	0.04*
	WM	612335 (11230)	540237 (12064)	<0.001*
	GM	427508 (6492)	399274 (6975)	0.006*
	RHip	3602 (106)	2932 (114)	<0.001*
	LHip	3591 (99)	2822 (107)	<0.001*
	LThal	7013 (109)	6433 (118)	0.001*
	RThal	6808 (109)	6371 (117)	0.011*
	LAmy	1256 (41)	1054 (44)	0.002*
	RAmy	1323 (63)	1120 (66)	0.035*

Volumes of different brain structures expressed in mm^3. Values are expressed as mean (SD). Significance was set at p = 0.050. * refers to statistically significant values.

Table 3: Spinal cord morphometric changes in AD patients

	Vertebra	HC (n=32)	AD (n=28)	p-value
		mean (SD)	mean (SD)	
Area (mm^2)	C1	69.8 (1.6)	63.1 (1.8)	0.009*
	C2	65.7 (1.3)	60.2 (1.4)	0.008*
	C3	62.5(1.4)	56.9 (1.6)	0.013*

	C4	62.5 (1.6)	57.2 (1.7)	0.031*
	C5	58.9 (1.6)	52.8 (1.7)	0.019*
	C2-C3	65.1 (1.6)	58.3 (1.7)	0.007*
Volume (mm^3)	C1	883.4 (27.3)	800.4 (29.3)	0.050*
	C2	979.8 (28.4)	857.1 (30.6)	0.006*
	C3	932.3 (29)	886.9 (31.2)	0.308
	C4	882.3 (35.1)	807.9 (37.7)	0.168
	C5	667 (34.5)	609.1 (37.1)	0.275
	C2-C3	1860.5 (66.8)	1729.9 (71.7)	0.204

Cross sectional area (in mm^2) and volumes (in mm^3) of spinal cord vertebrae. Values are expressed as mean (SD). Significance was set at p = 0.050. * refers to statistically significant values.

Table 4: Cerebral and spinal cord morphometric metrics

Set of all calculated Metrics				**Set of uncorrelated metrics**			
Brain	**Spine**		**Personal**	**Brain**	**Spine**		**Personal**
WM	CSA1	CSV1	Age	WM	-	-	Age
GM	CSA2	CSV2	Gender	GM	-	-	Gender
RHip	CSA3	CSV3		LHip	-	CSV3	
LHip	CSA4	CSV4		RHip	-	-	
RThal	CSA5	CSV5		-	-	CSV5	
LThal	CSA23	CSV23		-	CSA23	-	
RAmy				-			
LAmy				LAmy			

Left column: initial dataset of morphometric metrics. Right column: subset of uncorrelated morphometric metrics. WM=white matter, GM=gray matter, RHip=right hippocampus, LHip=left hippocampus, RThal=right thalamus, LThal=left thalamus, RAmy=right amygdala, LAmy=left amygdala, CSA=cross sectional area, CSV=cross sectional volume

Table 5: Features ranking

Features	**Weight**
RHip	0.1125
WM	0.0630
LAmy	0.0629
LHip	0.0615
CSA23	0.0317
GM	-0.0041

9 HC and 9 AD patients were used in the ranking procedure. Ranking Algorithm: ReliefF applied on a dedicated subset (30% of instances, number of neighbors = 10).

Table 6: Random Forest classification

Performance	
Accuracy	76 %
Sensitivity	74%
Specificity	78%
Area Under Curve	86%

Feature	RF weight
LHip	9.039
RHip	2.734
LAmy	2.263
CSA23	1.828
WM	0.323
GM	0.060

23 HC and 19 AD were used to test classifier performance. A leave-one-out procedure was used to test the performance of Random Forest (RF) with the best feature subset reported in table 5. RF features weight are also reported.

Table 7: MMSE outcomes

Multiple Linear Model	Explained Variance	Influence Significance
$MMSE = \beta_1*LHip+\beta_2*RHip+\beta_3*LAmy+\beta_4*CSA23+\beta_5*GM+\beta_6*WM$	44%	<0.001
$MMSE = \beta_1*LHip+\beta_2*RHip+\beta_3*LAmy+\beta_4*GM+\beta_5*WM$	43%	<0.001
$MMSE = \beta_1*LHip+\beta_2*LAmy+\beta_3*GM+\beta_4*WM$	43%	<0.001
$MMSE = \beta_1*LHip+\beta_2*GM+\beta_3*WM$	42%	<0.001
$MMSE = \beta_1*LHip+\beta_2*WM$	40%	<0.001

Linear Model	Explained Variance	Influence Significance
$MMSE = \beta*WM$	36%	<0.001
$MMSE = \beta*LHip$	30%	<0.001
$MMSE = \beta*RHip$	22%	<0.001
$MMSE = \beta*GM$	17%	0.001
$MMSE = \beta*LAmy$	16%	0.001
$MMSE = \beta*CSA23$	13%	0.005

MMSE Linear Regression Models. The model-explained variance is calculated with the R^2 index. Significance was set to p=0.05; all described model showed statistically significant influence (ANOVA).

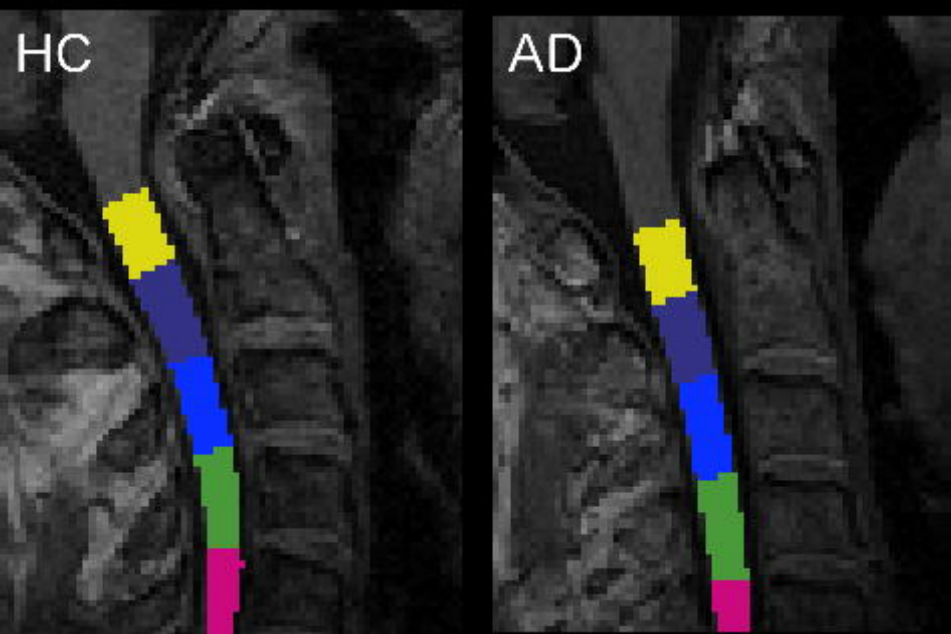
HC
AD

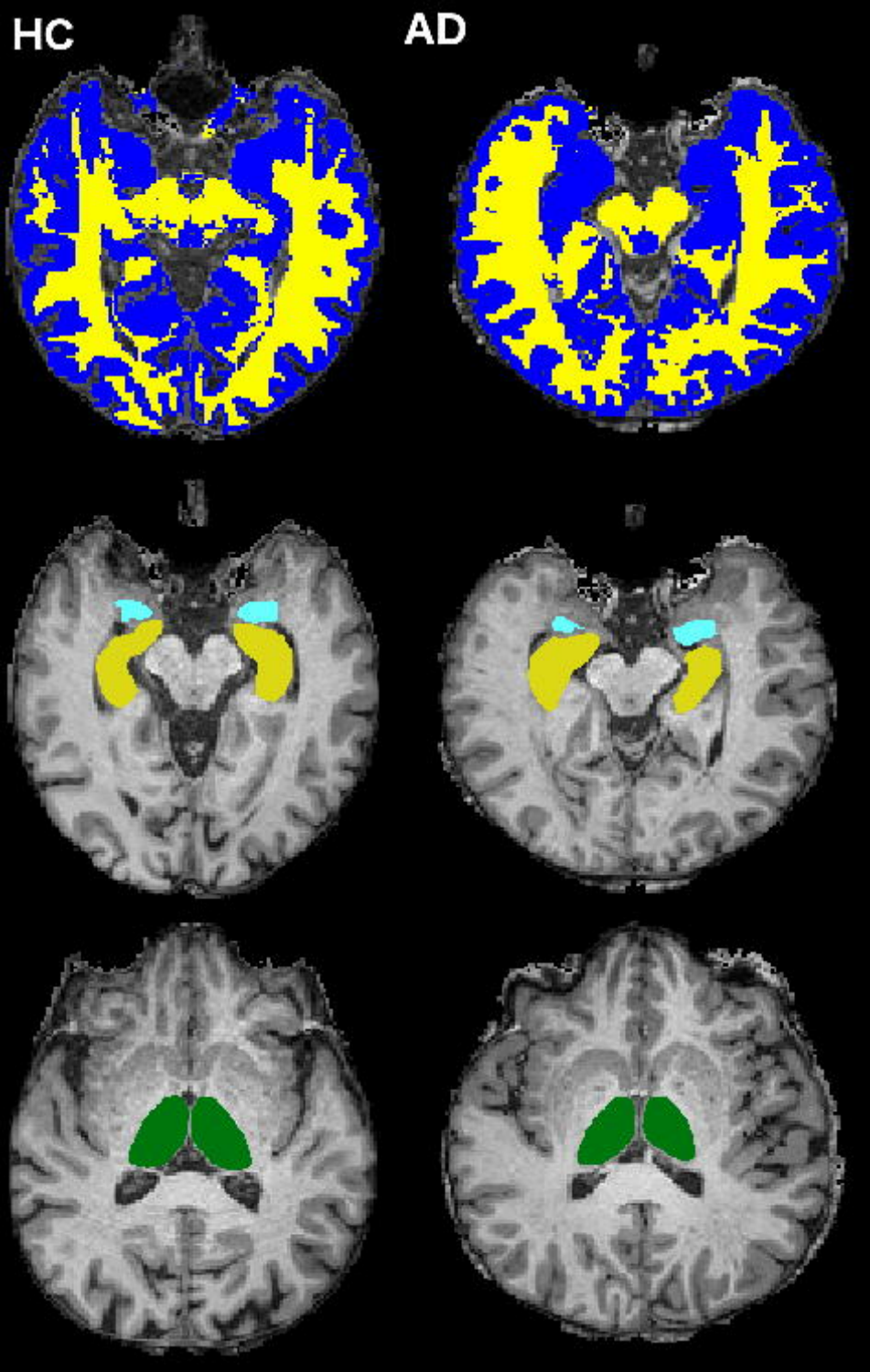
HC
AD

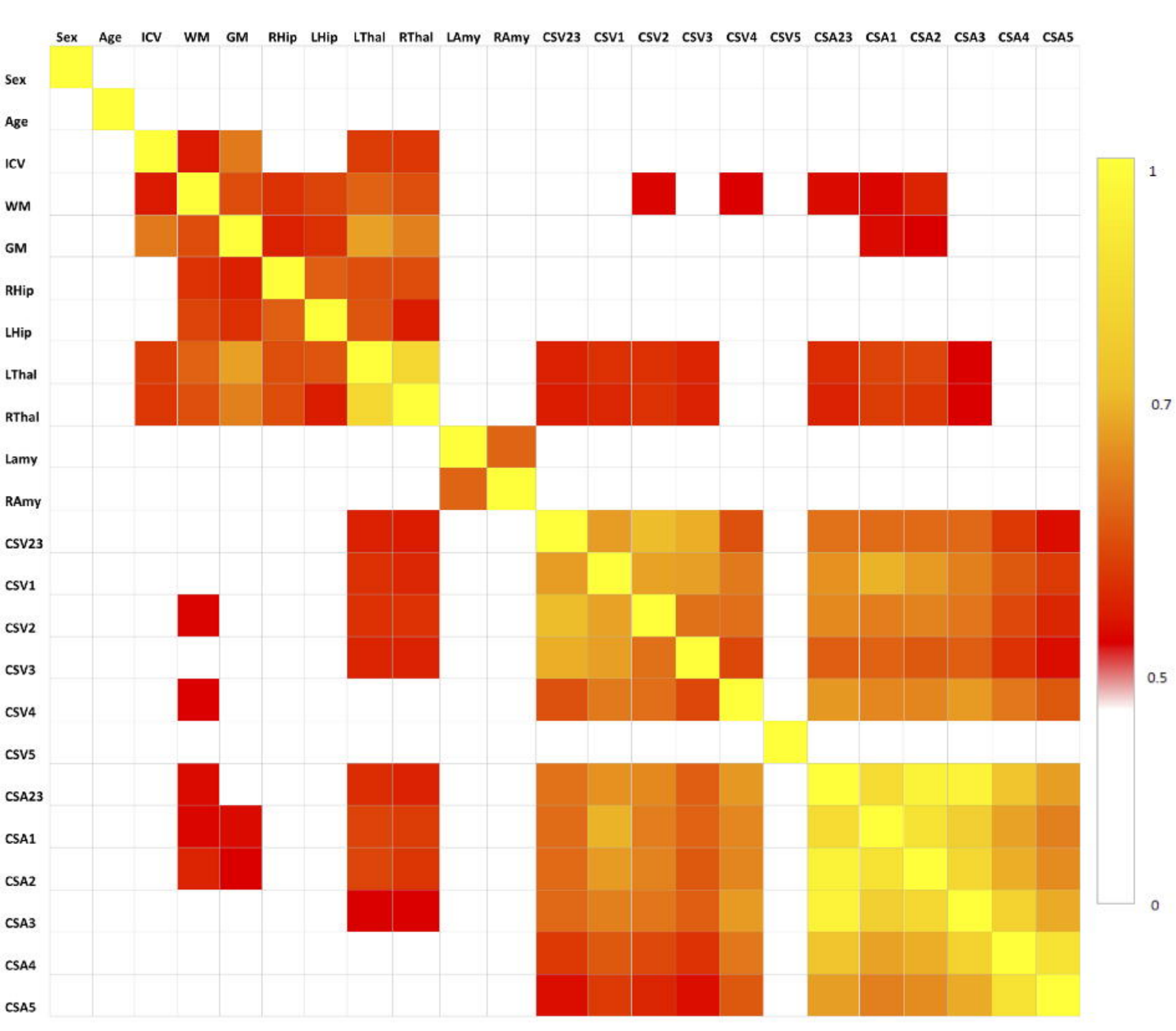
Sex
Age
ICV
WM
GM
RHip
LHip
LThal
RThal
LAmy
RAmy
CSV23
CSV1
CSV2
CSV3
CSV4
CSV5
CSA23
CSA1
CSA2
CSA3
CSA4
CSA5
1
0.7
0.5
0

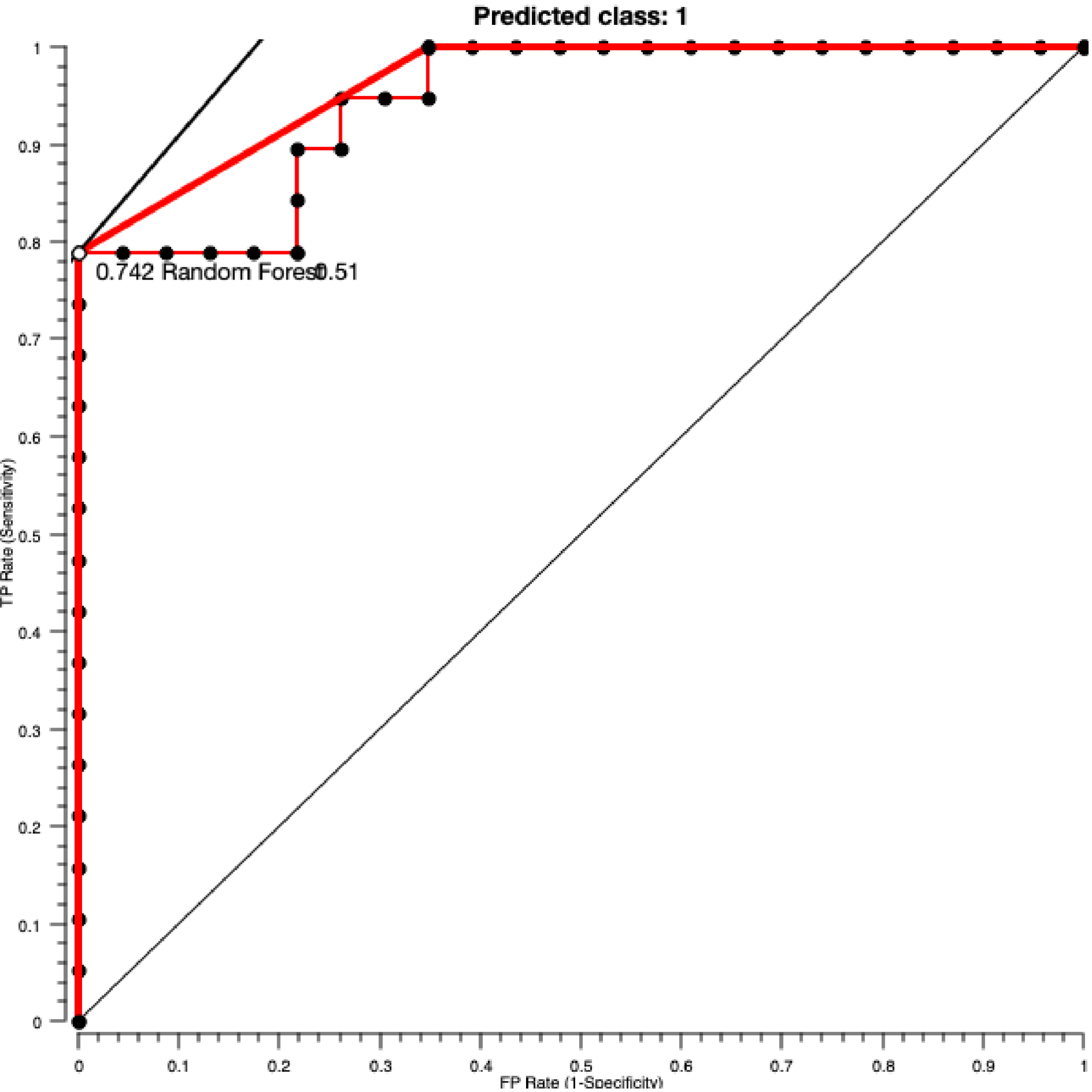
Predicted class: 1
0.742 Random Fores
0.51
TP Rate (Sensitivity)
FP Rate (1-Specificity)
0
0.1
0.2
0.3
0.4
0.5
0.6
0.7
0.8
0.9
1